Temperature-dependent concentration quenching of Nd^{3+} fluorescence in fluoride glasses

1994 J. Phys.: Condens. Matter 6 913

(http://iopscience.iop.org/0953-8984/6/4/011)

J. Phys.: Condens. Matter 6 (1994) 913–924. Printed in the UK

Temperature-dependent concentration quenching of Nd^{3+} fluorescence in fluoride glasses

R Balda†, J Fernández†, A Mendioroz†, J L Adam‡ and B Boulard§

† Departamento de Física Aplicada I, Escuela Técnica Superior de Ingenieros Industriales y de Telecomunicación, Universidad del País Vasco, Alameda de Urquijo s/n 48013 Bilbao, Spain

‡ Laboratoire de Verres et Céramiques, UA CNRS 1496, Université de Rennes, Campus de Beaulieu, 35042 Rennes Cédex, France

§ Laboratoire des Fluorures, UA CNRS 449, Faculté des Sciences, Université du Maine, 72017 le Mans Cédex, France

Received 15 June 1993, in final form 5 October 1993

Abstract. The optical properties and temperature-dependent concentration quenching of Nd^{3+} fluorescence have been investigated in heavy-metal and transition-metal fluoride glasses using steady-state and time-resolved laser spectroscopy. Judd–Ofelt parameters were derived from the absorption spectra and used to calculate the $^4F_{3/2} \rightarrow {}^4I_{11/2}$ stimulated-emission cross-section and the $^4F_{3/2}$ radiative lifetime. From the thermal behaviour of lifetimes, a T^3 dependence for the non-radiative Nd–Nd relaxation processes has been found in the 15–100 K temperature range for the three families of fluoride glasses investigated, which is in agreement with a two-site non-resonant process.

1. Introduction

Fluoride glasses have been a subject of increasing interest in many aspects. Most of the investigations of fluoride glasses have been motivated by the aim of developing ultralow-loss optical fibres in the mid-infrared (IR). Among the potential uses related to the passive optical behaviour, there are other important applications when these glasses are doped by rare-earth ions. Their relatively far IR edge, their ability to incorporate significant numbers of transition-metal ions and rare-earth ions into the glass and their high emission efficiency, due to multiphonon emission rates lower than other glasses, make them privileged candidates for laser applications [1 and references therein]. Laser action has been reported previously on rare-earth-doped heavy-metal fluoride glasses, both in bulk and fibre form [2–6]. The lasing properties of Nd^{3+} have been reported in fluorozirconate glasses in a fibre configuration [5] and in bulk form [6] pumped by another laser. Recently, laser action has been proved in an Nd^{3+}-doped Ba–In–Ga fluoride glass in bulk form, pumped by flashlamps [7].

It is known that a knowledge of the spectroscopic properties of Nd^{3+} ions is of fundamental importance for laser action [8]. These properties include absorption and emission cross-sections, peak wavelengths and linewidths, lifetimes and quantum efficiencies, and fluorescence-quenching processes. For a good efficiency, fluorescence lifetimes of Nd^{3+} ions must be close to the calculated radiative lifetime. The lifetime of an excited state is determined by all the competing radiative and non-radiative decay processes; the later include both Nd–Nd self-quenching and multiphonon relaxation. Concentration quenching and multiphonon emission are dependent on the lasing ion and the glass hosts [9]. In a previous work [10], some of the present authors studied the luminescence quenching

0953-8984/94/040913+12$07.50

of the $^4F_{3/2} \rightarrow {}^4I_{11/2}$ laser transition in a Ba–In–Ga fluoride glass, by investigating the thermal and concentration dependence of lifetimes. Although multiphonon relaxation of the $^4F_{3/2}$ state is negligible for fluoride glasses, at a concentration higher than 1 mol% the experimental lifetime was shorter than the predicted radiative lifetime even at He temperature. From the thermal behaviour of lifetimes, a T^3 dependence for the non-radiative Nd–Nd relaxation in the 15–100 K temperature range was found. The aim of this work is to investigate this concentration–temperature dependence of the lifetimes of Nd^{3+} ions in three families of heavy-metal and transition-metal fluoride glasses. As we shall see, we have found a similar behaviour in all cases for the non-radiative Nd–Nd relaxation, which could correspond to a two-site non-resonant process in the short-wavelength regime as has been shown by Holstein *et al* [11].

2. Experimental details

Heavy-metal fluoride glass samples doped with various concentrations of Nd (0.1, 1, 2, 3, and 5 mol%) were prepared at the University of Rennes (France), and transition-metal fluoride glasses doped with 0.1, 1, and 3 mol% of Nd were prepared at the University of Maine (France).

The molar compositions of the samples studied are given in table 1. The experimental method for preparing the glasses has been well described in the literature [12, 13].

Table 1. Chemical compositions of glasses used in this work.

Glass	Composition (mol%)
ZBLAN	$58ZrF_4$–$18BaF_2$–$5.5LaF_3$–$3AlF_3$–$15NaF$
BIGaZYTZr	$30BaF_2$–$18InF_3$–$20ZnF_3$–$10YF_3$–$6ThF_4$–$12GaF_3$–$4ZrF_4$
PZG	$38PbF_2$–$20ZnF_2$–$35GaF_3$–$2InF_3$–$2CdF_2$–$3LaF_3$

The sample temperature was varied between 4.2 and 300 K with a continuous-flow cryostat. Conventional absorption spectra were performed with a CARY 5 spectrophotometer. The emission measurements were made using an Ar laser as exciting light. The fluorescence was analysed with a 0.22 m SPEX monochromator, and the signal was detected by a Hamamatsu R7102 extended IR photomultiplier and finally amplified by a standard lock-in technique.

Lifetime measurements were performed with a tunable dye laser (1 ns pulse width) and the emission detected with a Hamamatsu R7102 photomultiplier. The data was processed by an EGG-PAR boxcar integrator.

3. Spectroscopic results

3.1. Absorption properties

The room-temperature absorption spectra were recorded for all samples in the 300–2600 nm spectral range. Figure 1 shows the absorption coefficient for the samples with 1 mol% of Nd^{+3} in the 300–900 nm range. Data from these spectra can be used to calculate the radiative lifetime of the $^4F_{3/2}$ excited J manifold, the branching ratios and the radiative transition probabilities of fluorescence transitions to the lower-lying ^4I_J manifolds, according to the

Judd-Ofelt (JO) theory [14, 15]. The oscillator strengths of the absorption bands lying between 350 nm and 2500 nm and originating from the $^4I_{9/2}$ ground state were calculated for the samples with an Nd^{3+} concentration of 1 mol%, using the expression

$$f = \frac{mc^2}{\pi e^2 N} \frac{2.303}{d} \int \frac{\mathrm{OD}(\lambda)\, \mathrm{d}\lambda}{\lambda^2} \tag{1}$$

where m and e are the electron mass and charge respectively, c is the velocity of light, $\mathrm{OD}(\lambda)$ the optical density, and d the sample thickness.

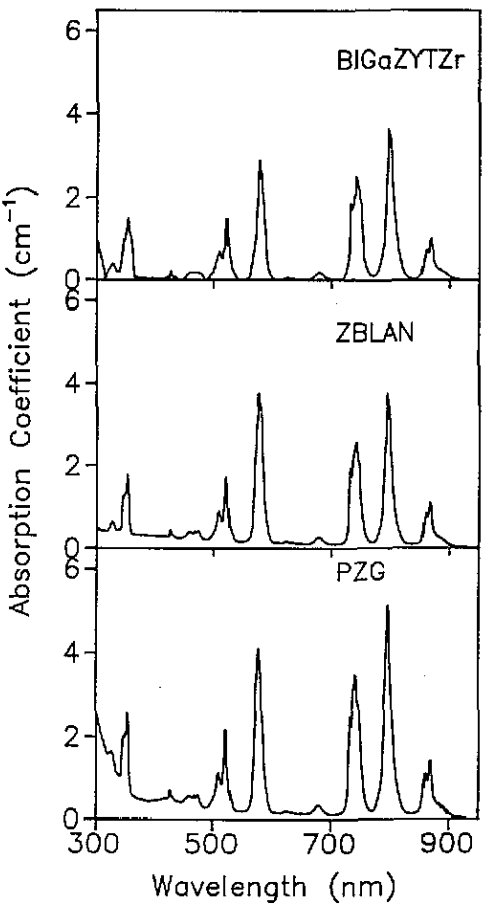

Figure 1. Room-temperature absorption spectra of Nd^{3+} ions in the three glasses doped with 1 mol%.

The experimental f values have been used to calculate the Ω_t parameters corresponding to the JO theory. Using this theory, the line strength of electric-dipole transitions between J initial $|(S, L)J\rangle$ and terminal $|(S', L')J'\rangle$ manifolds may be written in the form [16]

$$S = \sum_{t=2,4,6} \Omega_t \left| \langle (S', L')J' \| U^{(t)} \| (S, L)J \rangle \right|^2 \tag{2}$$

Table 2. Measured (f_m) and calculated (f_c) absorption line strengths for Nd^{3+} (1 mol%) in the three glasses.

Transition	λ (nm)	$f_m \times 10^8$	$f_c \times 10^8$	dif $\times 10^8$
BIGaZYTZr				
$^4I_{9/2} \rightarrow {}^4I_{13/2}$	2502.0	110.70	108.31	2.39
$^4I_{15/2}$	1649.0	22.82	16.01	6.81
$^4F_{3/2}$	869.4	136.63	141.04	−4.41
$^4F_{5/2}$, $^2H_{9/2}$	797.9	508.06	501.27	6.79
$^4F_{7/2}$, $^4S_{3/2}$	740.9	516.53	545.02	−28.49
$^4F_{9/2}$	679.3	36.83	40.51	−3.68
$^4G_{5/2}$, $^2G_{7/2}$	577.1	775.83	783.27	−7.44
$^2K_{13/2}$, $^4G_{7/2}$, $^4G_{9/2}$	516.9	436.31	346.29	90.02
$^2K_{15/2}$, $^2G_{9/2}$, $^2D_{3/2}$, $^4G_{11/2}$	466.7	116.73	84.92	31.81
$^2P_{1/2}$, $^2D_{5/2}$	427.1	32.51	39.17	−6.66
ZBLAN				
$^4I_{9/2} \rightarrow {}^4I_{13/2}$	2494.0	99.80	111.18	−11.4
$^4I_{15/2}$	1660.0	22.80	16.23	6.57
$^4F_{3/2}$	868.2	140.30	155.40	−15.1
$^4F_{5/2}$, $^2H_{9/2}$	797.1	541.00	527.73	13.3
$^4F_{7/2}$, $^4S_{3/2}$	740.8	538.10	559.34	−21.2
$^4F_{9/2}$	678.4	33.60	42.25	−8.66
$^4G_{5/2}$, $^2G_{7/2}$	576.5	1165.9	1170.2	−4.32
$^2K_{13/2}$, $^4G_{7/2}$, $^4G_{9/2}$	516.6	450.6	399.45	51.2
$^2K_{15/2}$, $^2G_{9/2}$, $^2D_{3/2}$, $^4G_{11/2}$	465.6	134.5	91.48	43.00
$^2P_{1/2}$, $^2D_{5/2}$	427.8	44.60	43.88	0.71
PZG				
$^4I_{9/2} \rightarrow {}^4I_{13/2}$	2494.0	76.90	142.15	−65.3
$^4I_{15/2}$	1660.0	21.22	20.90	0.31
$^4F_{3/2}$	866.0	147.33	179.66	−32.3
$^4F_{5/2}$, $^2H_{9/2}$	796.5	666.00	651.69	14.3
$^4F_{7/2}$, $^4S_{3/2}$	741.5	657.80	713.07	−55.3
$^4F_{9/2}$	678.5	44.70	52.65	−8.58
$^4G_{5/2}$, $^2G_{7/2}$	576.5	975.23	983.97	−8.74
$^2K_{13/2}$, $^4G_{7/2}$, $^4G_{9/2}$	515.9	542.40	443.88	98.5
$^2K_{15/2}$, $^2G_{9/2}$, $^2D_{3/2}$, $^4G_{11/2}$	469.0	184.23	108.6	76.6
$^2P_{1/2}$, $^2D_{5/2}$	427.1	32.27	49.24	−17.0

where Ω_t are the JO intensity parameters. It is known that the reduced matrix elements, $\langle \| U^t \| \rangle$, are almost independent of the ion environment. We have used the values reported by Carnall *et al* [17] for Nd^{3+} ions in LaF_3.

The oscillator strength of a transition can be written as

$$f = [8\pi^2 m\nu/3h(2J+1)][(n^2+2)^2/9n]S \tag{3}$$

where m is the electron mass, ν is the frequency of the transition, J is the total angular momentum of the initial level ($J = \frac{9}{2}$ in Nd^{3+}), and n is the refractive index. The best set of Ω_t parameters can be determined by a least-squares fitting of the calculated f values given by (3) to the experimental ones. The quality of the fit obtained from the absorption spectra is shown in table 2 where f_m is the measured absorption line strength and f_c is that calculated using Judd's theory [14]. The JO parameters obtained from this fitting are displayed for the three glasses in table 3. These values are in good agreement with those previously reported for the Nd^{3+} ion in different glass matrices [18–24].

Table 3. JO parameters calculated from the absorption spectra for Nd^{3+} (1%).

JO parameters (10^{-20} cm^2)	BIGaZYTZr	ZBLAN	PZG
Ω_2	1.31	2.66	1.53
Ω_4	2.71	3.05	3.19
Ω_6	4.01	4.08	4.93
Spectroscopic quality factor (Ω_4/Ω_6)	0.67	0.75	0.65

Table 4. Radiative-property parameters for the $^4F_{3/2} \rightarrow {}^4I_J$ ($J = \frac{9}{2}, \frac{11}{2}, \frac{13}{2}, \frac{15}{2}$) transitions of Nd^{3+} (1 mol%) in the three fluoride glasses studied.

Transition	BIGaZYTZr		ZBLAN		PZG	
$^4F_{3/2} \rightarrow$	A (s^{-1})	β_R	A (s^{-1})	β_R	A (s^{-1})	β_R
$^4I_{15/2}$	9.9	0.005	10.5	0.0005	14.9	0.0056
$^4I_{13/2}$	195.4	0.105	200.5	0.100	285.7	0.1073
$^4I_{11/2}$	950.6	0.511	1009.3	0.504	1398.3	0.525
$^4I_{9/2}$	704.0	0.379	782.0	0.391	961.5	0.361
W_R (s^{-1})	1859.9		2002.2		2660.5	

The spontaneous emission probabilities from the $^4F_{3/2}$ to the ^4I_J ($J = \frac{15}{2}, \frac{13}{2}, \frac{11}{2}, \frac{9}{2}$) can be calculated from the Ω_t parameters. The radiative transition probability from the initial J' manifold $|(S', L')J'\rangle$ to the terminal manifold $|(S, L)J\rangle$ is given by [16]

$$A[(S', L')J'; (S, L)J] = \frac{64\pi^4 e^2}{3h(2J'+1)\lambda^3} n \frac{(n^2+2)^2}{9} \sum_{t=2,4,6} \Omega_t \left|\langle (S', L')J' \| U^{(t)} \| (S, L)J \rangle\right|^2 \tag{4}$$

where $n(n^2+2)^2/9$ is the local-field correction for the Nd^{3+} ion in the initial J' manifold, n is the refractive index, λ is the wavelength of the transition, and J is the terminal manifold.

The radiative lifetime is related to the radiative transition probability by [16]

$$\tau_R = \left(\sum_{S,L,J} A[(S', L')J'; (S, L)J] \right)^{-1} . \tag{5}$$

The branching ratios can be obtained from the transition probabilities by using [16]

$$\beta[(S'L')J'; (S, L)J] = A[(S', L')J'; (S, L)J] \Big/ \sum_{S,L,J} A[(S', L')J'; (S, L)J]. \tag{6}$$

The radiative-transition probabilities and branching ratios for the fluorescence from the $^4F_{3/2}$ to the ^4I_J states are listed in table 4, together with the total spontaneous-emission probability (W_R). According to Jacobs and Weber [18], the intensity of the $^4F_{3/2} \rightarrow {}^4I_{11/2}$ laser transition is only dependent on the Ω_4 and Ω_6 parameters. For a large cross-section, Ω_4 and Ω_6 are required to be as large as possible. Since Ω_2 does not enter the branching ratios for the $^4F_{3/2}$ fluorescence, it can be expressed in terms of the Ω_4/Ω_6 ratio. To maximize the fluorescence intensity to $^4I_{11/2}$ one requires $\Omega_4 \ll \Omega_6$. From the values obtained for these glasses, the highest spectroscopic quality factor corresponds to the ZBLAN glass (see table 3).

3.2. Fluorescence properties

The $^4F_{3/2} \rightarrow {}^4I_{11/2}$ steady-state fluorescence spectrum at room temperature was measured for the three glasses with 1 mol% of Nd^{3+} by exciting the samples with an Ar laser. As an example figure 2 shows this emission spectrum for ZBLAN glass. Since the emission band is slightly asymmetric, an effective linewidth was determined by integrating the fluorescence lineshape and dividing by the intensity at the peak fluorescence emission wavelength [18]. The stimulated-emission cross-section can be determined from spectral parameters using [18]

$$\sigma_p(\lambda_p) = (\lambda_p^4/8\pi cn^2\Delta\lambda_{eff})A[(^4F_{3/2}); (^4I_{11/2})] \tag{7}$$

where λ_p is the peak fluorescence wavelength, n is the refractive index, $\Delta\lambda_{eff}$ is the effective linewidth of the transition and $A[(^4F_{3/2}); (^4I_{11/2})]$ is the radiative-transition probability for this transition.

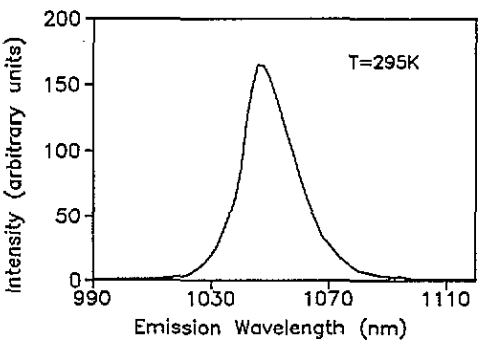

Figure 2. Room-temperature fluorescence spectrum of the $^4F_{3/2} \rightarrow {}^4I_{11/2}$ transition in ZBLAN:Nd^{3+}(1%) glass obtained under excitation with an Ar laser.

The stimulated-emission cross-section for the $^4F_{3/2} \rightarrow {}^4I_{11/2}$ transition is presented in table 5 together with the effective fluorescence linewidth.

Table 5. Room-temperature emission properties of Nd^{3+} (1 mol%) in the three fluoride glasses.

$^4F_{3/2} \rightarrow {}^4I_{11/2}$	BIGaZYTZr	ZBLAN	PZG
τ_R (μs)	537	499	375
τ_{exp} (μs)	409	430	296
λ_p (nm)	1048	1046	1048
$\Delta\nu_{eff}$ (cm^{-1})	229	218	230
σ_p ($\times 10^{20}$ cm^2)	2.68	2.9	3.5

3.3. Lifetime results

The decays of the $^4F_{3/2} \rightarrow {}^4I_{11/2}$ transition as a function of temperature were performed with a narrow-band tunable dye laser (1 ns pulse width), exciting the sample at the $^4I_{9/2} \rightarrow {}^4G_{5/2}$ absorption band (575 nm), in the 4.2–300 K range. The radiative lifetimes, calculated from

the absorption parameters and measured fluorescence lifetimes of the three glasses with 1 mol% of Nd^{3+}, are given in table 5.

The lifetime values as a function of temperature between 4.2 K and 300 K are presented in figure 3. The decays were found to be single exponentials at all temperatures As an example figure 4 shows the room-temperature logarithmic plot of the experimental decays for the three glasses with 3 mol% of Nd^{3+}.

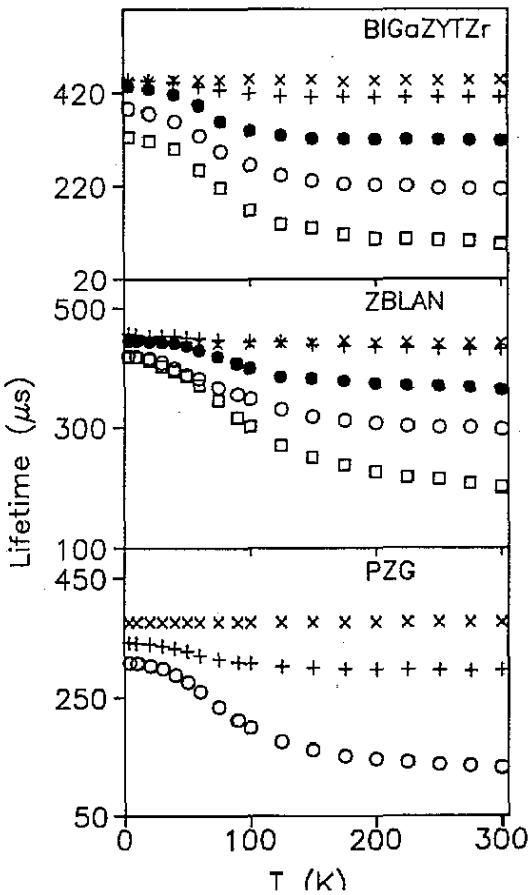

Figure 3. Temperature dependence of the $^4F_{3/2}$-state lifetime of Nd^{3+} ions in BIGaZYTZr, ZBLAN, and PZG glasses: ×, 0.1 mol%; +, 1 mol%; ●, 2 mol%; ○, 3 mol%; and □, 5 mol%. Lifetimes were obtained by exciting at 575 nm and collecting the fluorescence at the emission peak of the $^4F_{3/2} \rightarrow {}^4I_{11/2}$ transition.

4. Discussion

4.1. Absorption and equilibrium luminescence spectra

As can be seen in figure 3, at low temperatures and concentrations the lifetime nearly approaches the radiative lifetime, hence the rate of non-radiative decay by multiphonon

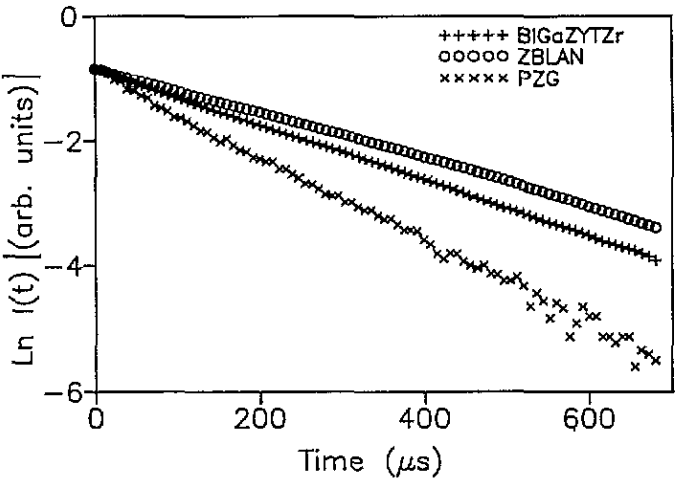

Figure 4. Logarithmic plot of the fluorescence decays of the $^4F_{3/2}$ state for the three glasses doped with 3 mol% of Nd^{3+}. The decays were obtained by exciting at the $^4I_{9/2} \rightarrow {}^4G_{5/2}$ absorption band and monitored at 1048 nm. Data correspond to 300 K.

emission must be small. In these glasses the multiphonon relaxation rate for the $^4F_{3/2}$ manifold is expected to be small because of the high energy gap to the next-lower-lying J manifold and the typical values of phonon energies involved [10]. As concentration rises the decays remain single exponential but a decrease in the experimental lifetimes is observed even at He temperature. This behaviour could be associated with a rapid energy diffusion between Nd^{3+} ions that can lead to a spatial equilibrium within the Nd^{3+} system. In the transfer rapid limit the donor transfer takes place so quickly that transfer times for different donor–acceptor pairs are averaged out and the whole system exhibits a simple exponential decay as is experimentally observed [25, 26]. In order to investigate the energy-migration process we have analysed the relation between the absorption and equilibrium luminescence spectra. If the diffusion rate greatly exceeds that of the excited-state decay, then, during a time equal to the lifetime of ions in the metastable level, thermodynamical equilibrium of the energy distribution of the excitations of the inhomogeneous ensemble of centres will be reached. The actual pattern of this distribution, $\rho(E, T, Z)$, and of the corresponding luminescence spectra depends neither on the excitation method nor on the migration parameters. It is only governed by the density of states $g(E)$, the temperature, and the fraction of excited centres Z [27]. In the limit of high temperature or low density, where the number of available quantum states is much greater than the number of centres, the distribution becomes a Boltzmann distribution and the equilibrium temperature can be obtained from the slope $\ln[\rho(E)/g(E)]$. Figure 5 shows the relation between the Nd^{3+} absorption and luminescence spectra for the $^4I_{9/2} \leftrightarrow {}^4F_{3/2}$ transition in BIGaZYTZr: 1 mol% Nd^{3+}. The absorption cross-section was taken to be proportional to $g(E)$ and the luminescence band profile proportional to $\rho(E)$ (profile areas being normalized). The temperature derived from the slope calculation, taking account of the branching ratio for the $^4F_{3/2} \rightarrow {}^4I_{9/2}$ transition, was 300 K, which agrees with the experimental temperature and demonstrates that the energy-migration process drives the system of excited centres to thermal equilibrium.

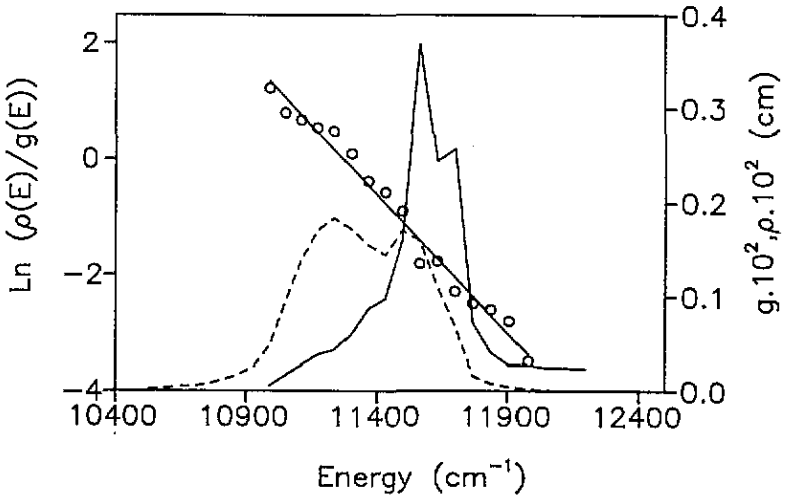

Figure 5. Relation between the Nd^{3+} (1 mol%) absorption and luminescence spectra in BIGaZYTZr glass: Solid line, $^4I_{9/2} \rightarrow {}^4G_{5/2}$ absorption band profile; dashed line, $^4F_{3/2} \rightarrow {}^4I_{9/2}$ luminescence band profile; O, $\ln[\rho(E)/g(E)]$. $T = 300$ K.

4.2. Temperature-dependent concentration quenching of Nd^{3+} fluorescence

As is well known 4f–4f transitions of trivalent rare-earth ions in first order are forbidden by Laporte's rule. The transitions observed are the result of parity mixing between 4f and 5d configurations originating from the odd crystal-field terms. At high enough Nd concentrations there could be some overlapping between the 4f configurations of one ion and the 5d configuration of its next neighbour, which could enhance the transition probability. In our case, the oscillator-strength measurements of the $^4I_{9/2} \rightarrow {}^4F_{3/2}$ transition for all the samples studied failed to show any dependence on Nd concentration within experimental error. The aforementioned facts therefore simplify the interpretation of the lifetime behaviour. The lifetime of the $^4F_{3/2}$ state of the Nd^{3+} ion in the doped glasses should be governed by the sum of probabilities for several competing processes such as radiative decay, non-radiative decay by multiphonon emission, and energy transfer to other Nd^{3+} ions. If one assumes that the purely radiative lifetimes τ_R of $^4F_{3/2}$ levels are independent of Nd concentration and temperature, and disregards multiphonon relaxation processes, the variations of the experimental lifetimes can be related to the non-radiative Nd–Nd relaxation processes by the simple relation

$$\tau_{exp}^{-1} = \tau_R^{-1} + W_{Nd\text{-}Nd}(T). \tag{8}$$

Figure 6 shows the decay rates of the three sample families for different Nd^{3+} concentrations at room, liquid-nitrogen, and liquid-helium temperatures. An outstanding result is that the decay rates are nearly linearly dependent on concentration at low temperatures. This result has also been interpreted by other authors as a demonstration of the existence of fast diffusion processes [28, 29].

A detailed study of the thermal dependence of lifetimes was presented in figure 3. These results suggest the presence of a fairly strong thermal quenching mechanism between 15 K and 100 K. If we disregard the multiphonon relaxation processes, relaxation via fast Nd–Nd diffusion processes and subsequent de-excitation via energy sinks should be

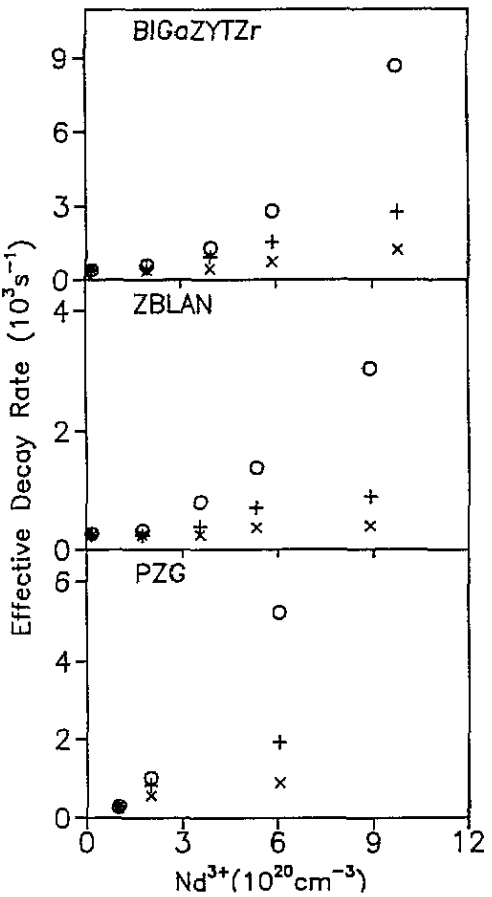

Figure 6. Effective decay rates as a function of concentration at different temperatures for the three glasses: ×, 4.2 K; +, 77 K; and ○, 300 K.

taken into account, as they occur even at low temperatures. Figure 7 shows the plot of $[W_{Nd\text{-}Nd}(T) - W_{Nd\text{-}Nd}(0)]^{1/3}$ in the 15–100 K range for the three glasses doped with 3 mol% of Nd^{3+}. It is worth noticing the good fit of $W_{Nd\text{-}Nd}$ to a T^3 dependence. This result also holds for all the measured concentrations higher than 0.5 mol%. As already pointed out in [10] this could correspond to a two-site non-resonant process in the short-wavelength regime as has been shown by Holstein *et al* [11]. In this process, the phonon emission and absorption take place at different sites, the ion–phonon interaction acts twice, and the site–site Hamiltonian once. This phonon-assisted excitation transfer between different states of similar ions could be understood by considering a small spread in the energy values of $^4F_{3/2}$ transitions to the J multiplicity, due to the inherent disorder of the glass structure. Two-phonon-assisted processes can dominate because the one-phonon-assisted process vanishes if energy mismatch ΔE is small. Moreover, a T^3 dependence implies that the transfer rate does not depend on ΔE. In agreement with this fact, the same T^3 behaviour has been observed for the three different families of fluoride glasses studied. In contrast, a recent investigation on fluorophosphate glasses with a high content of fluoride ions [30] failed to show the same temperature dependence.

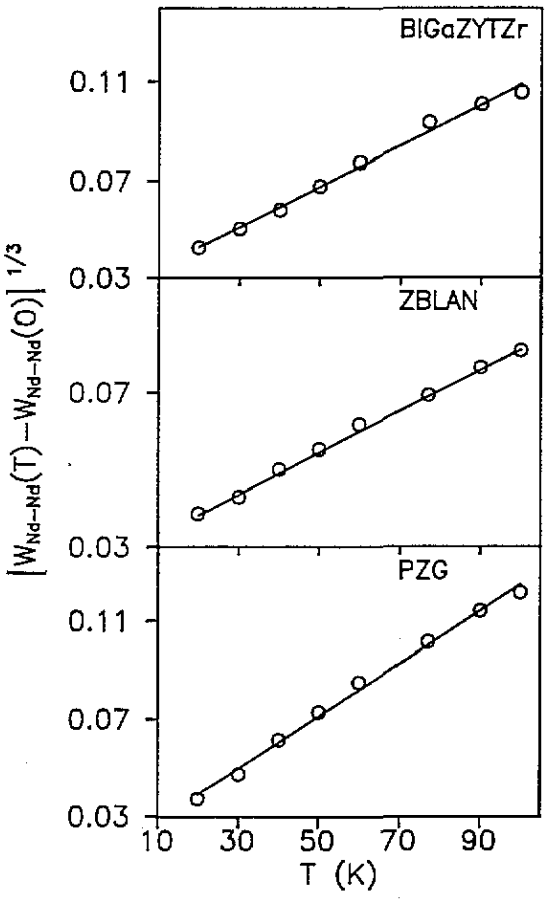

Figure 7. Plot of the non-radiative Nd–Nd relaxation rate in the 15–100 K temperature range for the three glasses doped with 3 mol% of Nd^{3+}. Symbols represent the experimental values, and solid lines are the fit to a T^3 dependence.

5. Conclusions

(i) From the steady-state optical absorption measurements the Judd-Ofelt parameters were derived and used to calculate the $^4F_{3/2} \rightarrow {}^4I_{11/2}$ stimulated-emission cross-section and the $^4F_{3/2}$ radiative lifetime for Nd^{3+} in heavy-metal (BIGaZYTZr, ZBLAN) and transition-metal (PZG) fluoride glasses. The calculated $^4F_{3/2}$ fluorescence branching ratios for all glasses were similar.

(ii) The emission lifetimes from the $^4F_{3/2}$ state are single exponential for all samples. As the concentration rises the decay remains single exponential but a decrease in the experimental lifetime is observed even at He temperature indicating that relaxation via fast Nd–Nd diffusion processes occurs.

(iii) From the relation between the absorption and luminescence spectra, the temperature of thermodynamical equilibrium of the energy distribution of the excitations has been estimated. The result obtained is in agreement with the true experimental temperature, demonstrating that the energy-migration process drives the system of excited centres to thermal equilibrium.

(iv) The luminescence thermal quenching of the $^4F_{3/2} \rightarrow {}^4I_{11/2}$ transition has been investigated from the thermal behaviour of lifetimes, and a T^3 dependence for the non-radiative Nd–Nd relaxation processes has been found in the 15–100 K temperature range for all the samples studied with Nd concentrations greater than 0.5 mol%, which is in agreement with a two-site non-resonant process.

Acknowledgments

This work was supported by the Comisión Interministerial de Ciencia y Tecnología (CICYT) of the Spanish Government (Ref. MAT93-0434), and the Basque Country Government (Ref. PGV 9215).

References

[1] Lucas J and Adam J L 1989 *Glastechnische Berichte* **62** 422
[2] Pollack S A and Robinson M 1988 *Electron Lett.* **24** 320
[3] Auzel F, Meichenin D and Poignant H 1988 *Electron Lett.* **24** 909
[4] Brierly M C, France P W and Millar C A 1988 *Electron Lett.* **24** 539
[5] Brierly M C and France P W 1987 *Electron Lett.* **24** 815
[6] Petrin R R, Kliewer M L, Beasley J T, Powell R C, Aggarwal I D and Ginther R C 1991 *IEEE J. Quantum Electron.* **QE-27** 1031
[7] Azkargorta J, Iparraguirre I, Balda R, Fernández J, Dénoue E and Adam J L *IEEE J. Quantum Electron.* submitted
[8] Weber M J 1990 *J. Non-Cryst. Solids* **123** 208
[9] Stokowski S E 1987 *Laser Spectroscopy and New Ideas* (Berlin: Springer) pp 47–88
[10] Elejalde M J, Balda R, Fernández J, Macho E and Adam J L 1992 *Phys. Rev.* B **46** 5169
[11] Holstein T, Lyo S K and Orbach M 1981 *Laser Spectroscopy of Solids* vol 49, ed W M Yen and P M Selzer (Berlin: Springer) pp 39–80
[12] Drexhage M G 1985 *Treatise on Materials Science and Technology* vol 26, ed M Tomozawa and R H Doremus (New York: Academic) pp 151–243
[13] Auriault N, Guery J, Mercier A M, Jacoboni C and De Pape R 1985 *Mater. Res. Bull.* **20** 309
[14] Judd B R 1962 *Phys. Rev.* **127** 750
[15] Ofelt G S 1962 *J. Chem. Phys.* **37** 511
[16] Krupke W F 1974 *IEEE J. Quantum Electron.* **QE-10** 450
[17] Carnall W T, Crosswhite H and Crosswhite H M 1977 *Argonne National Laboratory Report*
[18] Jacobs R R and Weber M J 1976 *IEEE J. Quantum Electron.* **QE-12** 102
[19] Reisfeld R and Jørgensen C K 1977 *Lasers and Excited States of Rare Earths* (Berlin: Springer) p 111
[20] Brecher C, Riseberg L A and Weber M J 1978 *Phys. Rev.* B **18** 5799
[21] Weber M J 1981 *Laser Spectroscopy of Solids (Topics in Applied Physics 49)* ed W M Yen and P M Selzer (Berlin: Springer) pp 189–239
[22] Lucas J, Chanthanasinh M, Poulain M, Poulain M, Brun P and Weber M J 1978 *J. Non-Cryst. Solids* **27** 273
[23] Reisfeld R, Eyal M, Jørgensen C K, and Jacoboni C 1986 *Chem. Phys. Lett.* **129** 392
[24] Tesar A, Campbell J, Weber M, Weinzapfel C, Lin Y, Meissner H and Toratani 1992 *Opt. Mater.* **1** 217
[25] Huber D L 1981 *Laser Spectroscopy of Solids* (reference 41) vol 49, ed W M Yen and P M Selzer (Berlin: Springer) p 83
[26] Weber M J 1971 *Phys. Rev.* **4** 2932
[27] Basiev T T, Malyshev V A and Przhevuskii A K 1987 *Spectroscopy of Solids Containing Rare-Earth Ions* vol 21, ed A A Kapliansky and R M Macfarlane (Amsterdam: North-Holland) p 275
[28] Voronko Y K, Mamedov T G, Osiko V V, Prokhorov A M, Sakun V P and Shcherbakov I A 1976 *Sov. Phys.–JETP* **44** 251
[29] Lenth W, Huber G and Fay D 1981 *Phys. Rev.* B **23** 3877
[30] Balda R, Fernández J, De Pablos A and Fernández-Navarro J M 1993 *Phys. Rev.* B **48** 2941